

Experimental and Approximate Analytical Modeling of Forced Convection from Isothermal Spheres

G. Refai Ahmed*

R—Theta Inc., Mississauga, Ontario L5T 1Y9, Canada

and

M. M. Yovanovich† and J. R. Culham‡

University of Waterloo, Waterloo, Ontario N2L 3G1, Canada

Forced convection heat transfer from isothermal spheres is examined over a wide range of Reynolds numbers, turbulence intensities, and Prandtl numbers using experimental and analytical techniques. An approximate analytical solution is presented that is based on a linearization of the thermal energy equation, for a full range of Prandtl numbers between zero and infinity, and for Reynolds numbers less than 10^5 . The experimental data presented in this study are confined to forced airflow with $Pr = 0.71$ and $3000 < Re_D < 50,000$. Results from the analytical solution are compared against data from the present experimental study plus data from other investigations published in the open literature. These comparisons reveal good agreement between experimental data and results from the current model.

Nomenclature

A	= surface area, m^2
b	= exponent in Eq. (1)
C_p	= specific heat, $J/kg \cdot K$
CR	= correction factor
$c_{\mathcal{L}}, C_{\mathcal{L}}$	= constants in Eq. (1)
D	= sphere diameter, m
h	= coefficient of convection heat transfer, $W/m^2 \cdot K$
K	= von Kármán's constant
k	= thermal conductivity, $W/m \cdot K$
L	= reference distance, m
\mathcal{L}	= arbitrary scale length, m
l	= mixing length, Ky , m
m	= exponent in Eq. (1)
Nu_D	= area-averaged Nusselt number, Dh/k
n	= exponent in Eq. (47)
Pr	= Prandtl number, ν/α
Q	= heat flow rate, W
q	= heat flux, W/m^2
Ra_D	= Rayleigh number, $g\beta\Delta TL^3/\alpha\nu$
Re_D	= Reynolds number, DV_∞/ν
$Re_D(\theta)$	= local Reynolds number, $DV(\theta)/\nu$
r, θ, ϕ	= spherical coordinates
Sc	= Schmidt number
Sh_D	= Sherwood number
T	= time mean-averaged temperature, K
T_∞	= freestream temperature, K
T^*	= nondimensional time mean-averaged
TF	= turbulence factor
Tu	= turbulence intensity, u'/V_∞
t	= time, s
\bar{u}	= time mean-average velocity, m/s
u'	= fluctuation velocity, m/s

V	= local velocity at edge of thermal boundary layer, m/s
V_∞	= freestream velocity, m/s
$V(\theta)$	= local velocity at edge of hydrodynamic boundary layer, m/s
\bar{v}_e	= area-averaged effective velocity, m/s
$v_e(\theta)$	= local effective velocity, m/s
$v_e^0(\theta)$	= local effective velocity $Pr \rightarrow 0$, m/s
$v_e^\infty(\theta)$	= local effective velocity $Pr \rightarrow \infty$, m/s
\bar{v}_e^0	= area-averaged effective velocity at $Pr \rightarrow 0$, m/s
\bar{v}_e^∞	= area-averaged effective velocity at $Pr \rightarrow \infty$, m/s
\bar{v}_r	= time mean-average velocity in radial direction, m/s
\bar{v}_θ	= time mean-average velocity in θ direction, m/s
X, Y, Z	= Cartesian coordinates
x, y	= local coordinates
x'	= distance from the end of the contraction area of the wind tunnel to the location of the test object, m
α	= thermal diffusivity, $k/C_p\rho$, m^2/s
α_t	= turbulent thermal diffusivity, m^2/s
α^*	= total thermal diffusivity, $\alpha + \alpha_t$, m^2/s
β	= thermal expansion, $1/K$
γ_D	= constant in Eq. (40)
$\Delta Nu/Nu$	= $(Nu_{Tu} - Nu_{Tu=0})/Nu_{Tu}$
δ	= local thickness of hydrodynamic boundary layer, m
δ_T	= local thickness of thermal boundary layer, m
δ_D^T	= displacement thickness of thermal boundary layer, m
δ_M^T	= momentum thickness of thermal boundary layer, m
ε	= surface emissivity
η	= similarity parameter, y/δ
ν	= kinematic viscosity, m^2/s
ν_t	= turbulent kinematic viscosity, m^2/s
ν^*	= total kinematic viscosity, $\nu + \nu_t$, m^2/s
ρ	= mass density, kg/m^3
Φ	= constant in Eq. (50), $K \cdot Tu \cdot \sqrt{Re_D}$

Subscripts

Conv	= convection
D	= displacement
e	= effective

Received Oct. 17, 1995; revision received Oct. 18, 1996; accepted for publication Oct. 30, 1996. Copyright © 1997 by the American Institute of Aeronautics and Astronautics, Inc. All rights reserved.

*Director, Advanced Thermal Engineering, 6220 Kestrel Road; currently at Nortel Technology International, P.O. Box 3511, Station C, Ottawa, Ontario K1Y 4H7, Canada.

†Professor, Microelectronics Heat Transfer Laboratory, Department of Mechanical Engineering, Fellow AIAA.

‡Research Associate Professor, Microelectronics Heat Transfer Laboratory, Department of Mechanical Engineering.

FC	= forced convection
M	= momentum
NC	= natural convection
Rad	= radiation
S	= surface
To	= total
W	= wire losses

Introduction

FORCED convection heat transfer from isothermal spheres is a fundamental heat transfer problem which has many industrial applications, such as boiling, air pollution, fermentation, and spray drying. Numerous experimental, analytical, and numerical studies have been conducted by researchers for the past 90 years. Most of the researchers presented their results in an area-averaged form as follows:

$$Nu_{\mathcal{G}} = c_{\mathcal{G}} + C_{\mathcal{G}} Re_{\mathcal{G}}^m Pr^b \quad (1)$$

where $c_{\mathcal{G}}$, $C_{\mathcal{G}}$, m , and b are constants.

Refai Ahmed and Yovanovich¹ reviewed various heat transfer correlations, found in previous studies, and found that most investigators agreed on the following: 1) the diffusive limit $Nu_D = 2.0$ for $Re_D \rightarrow 0$ and 2) the exponent on Pr is $b = \frac{1}{3}$.

In addition, Refai Ahmed and Yovanovich¹ concluded that the main reason for differences in the exponent on $Re_{\mathcal{G}}$ and $C_{\mathcal{G}}$ in the previous studies was because of the fitting of data over a different range of $Re_{\mathcal{G}}$, which produces different velocity profiles over the surface of the sphere.

Other studies have investigated the influence of freestream turbulence on flow and heat transfer over spheres. Loitzianski and Schwab² (this reference was used in Raithby³) examined the influence of turbulence intensity on the area-averaged Nusselt number for spheres. They found that increasing the turbulence intensity from about 0.5 to 3.0% increased Nu_D by 30% at $Re_D = 4 \times 10^4$ and by 36% at $Re_D = 1.2 \times 10^5$. Maisel and Sherwood⁴ also examined the effect of turbulence intensity on the mass transfer from spheres and found that increasing Tu from approximately 3.5 to 24% at $Re_D = 2.4 \times 10^3$ and 2×10^4 could cause an 18 and 25% increase in Nu_D , respectively. Rae and Pope⁵ proposed the following relationship to account for freestream turbulence:

$$V_{\infty} = TF \times V_{\infty(\text{measured})}$$

where TF was determined through experimental work. Clift et al.⁶ examined the effect of the turbulence intensity on the Nusselt number for spheres. They presented one equation for the relationship between $Nu_{\text{measured}}/Nu_{\text{corrected}}$ vs Reynolds number as follows:

$$\frac{Nu_{\text{measured}}}{Nu_{\text{corrected}}} = 1.0 + 4.8 \times 10^{-4} Re_D^{0.57}$$

Refai Ahmed⁷ developed the following general form for the freestream turbulence effect based on the correlation of Clift et al.⁶:

$$\begin{aligned} \frac{Nu_{\text{measured}} - Nu_{\text{corrected}}}{Nu_{\text{measured}}} &= \frac{\Delta Nu}{Nu} \\ &= \frac{0.253 + \ell_n Tu + 0.454 \ell_n Re_D}{26748.5 Re_D^{-0.723}} \quad (2) \end{aligned}$$

for

$$0.02 \leq Tu \leq 0.075$$

$$0.312 \times 10^4 \leq Re_D \leq 7.5 \times 10^4$$

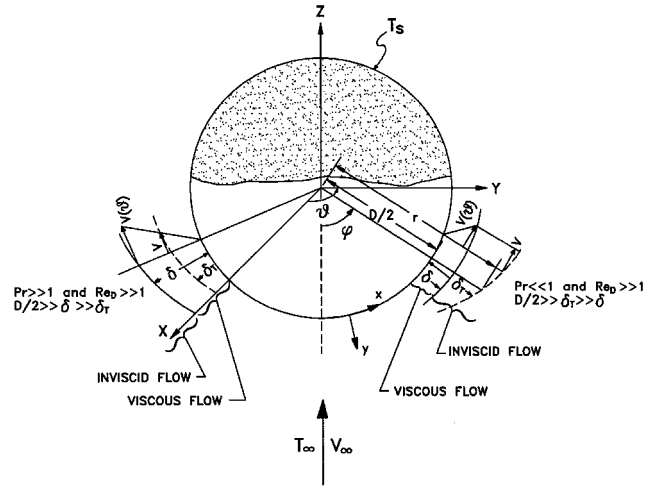


Fig. 1 Schematic diagram of the boundary layers over the sphere for $Pr \rightarrow \infty$ and $Pr \rightarrow 0$.

Although the area-averaged Nusselt number from spheres is known to increase with Tu , the precise relationship between Nusselt number and turbulence intensity is still not well established.

The objectives of the present investigation are to study the effect of turbulence intensity on heat transfer from spheres, as shown in Fig. 1, using both an experimental procedure and an approximate analytical method. This study will help provide an increased level of understanding into the determination of the appropriate value that should be used for the Reynolds number exponent found in Eq. (1). Finally, a general model for forced convection heat transfer from isothermal spheres will be developed.

Experimental Procedure and Results

The experimental test program was performed in a suction-type, open wind tunnel using a centrifugal fan located at the discharge. The working test section had dimensions $300 \times 300 \times 600$ mm. The operating velocity range of the wind tunnel was $0 < V_{\infty} < 14$ m/s (more details are given in Refai Ahmed¹⁰).

A 6061-T6 aluminum sphere with a diameter of 60 mm was suspended close to the test section outlet. The sphere was maintained isothermal with a maximum temperature variation of 0.5% at $V_{\infty} = 10.1$ m/s. Surface emittance measurements were also performed in a vacuum chamber based on an approach used by Hassani.⁸ Radiative heat transfer measurements were conducted in a vacuum chamber with the pressure maintained at 10^{-5} torr. The emissivity ϵ , was estimated to be 0.094 for the polished aluminum sphere. The maximum error and orthogonal error were 11.72 and 3.26%, respectively.

In addition, the steady-state convection heat loss from the sphere Q_{Conv} was obtained as follows:

$$Q_{\text{Conv}} = Q_{\text{To}} - Q_{\text{Rad}} - Q_{\text{W}} \quad (3)$$

where Q_{To} is the total power expended toward the Joulean heating of the sphere, Q_{Rad} is the radiation heat loss, and Q_{W} is the total conduction losses attributed to the thermocouple wires and the power leads. Mack⁹ and Refai Ahmed¹⁰ reported that the conduction losses for the same experimental setup were on the order of 0.5% of the total input power.

The turbulence intensity at the inlet and outlet of the test section are shown with respect to the Reynolds number in Fig. 2. The data at both the inlet and the outlet of the test section

have been correlated as function of Reynolds number, using a simple least-squares linear fit, as follows:

$$Tu = 1.5 \times 10^{-4} \cdot Re_D^{0.575} \text{ (inlet)} \quad (4)$$

$$Tu = 9.5 \times 10^{-5} \cdot Re_D^{0.575} \text{ (outlet)}$$

The maximum and average differences between the experimental data at the outlet test section and Eq. (4) are 7 and 3%, respectively. The relationship between Tu and Re_D at the outlet of the test section can also be used to determine the turbulence intensity in the vicinity of the sphere, which was located near the outlet of the test section.

Recently, Yovanovich and Vanoverbeke¹¹ developed a mixed convection model based on the forced convection correlation of Yuge¹² and the free convection correlation of Raithby and Holland¹³ for spheres and $Pr = 0.71$. They also demonstrated for forced convection from a sphere that the dimensionless heat transfer rate by convection is the summation of the dimensionless heat transfer by conduction, free convection, forced convection, and CR (for opposing flow), where $CR = 0.86 - 2.86(Ra_D/Re_D^2)^{1/4}$. Furthermore, Steinberger and Treybal¹⁴ proposed a formula similar to Yovanovich and Vanoverbeke¹¹ for assisted flow. The present study uses the concept of Yovanovich and Vanoverbeke¹¹ to remove the effect of free convection from the data. Therefore, Q_{FC} can be approximated as follows:

$$Q_{FC} = Q_{Conv} - Q_{NC} \quad (5)$$

The free convection heat transfer, with radiation effects eliminated, can be obtained as follows:

$$Nu_D = 2.0 + \frac{0.589Ra_D^{1/4}}{[1 + (0.469/Pr)^{9/16}]^{4/9}} \quad (6)$$

This model was developed by Churchill¹⁵ and has been confirmed through the analytical study of Jafarpur.¹⁶

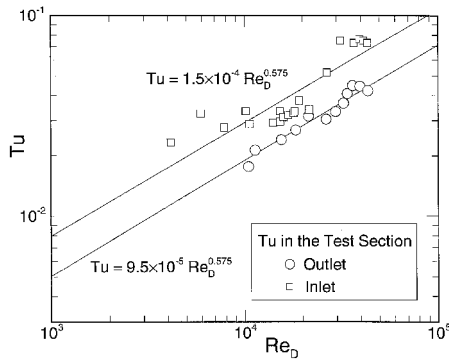


Fig. 2 Relationship between Tu and V_∞ at the inlet and the outlet of the wind-tunnel test section.

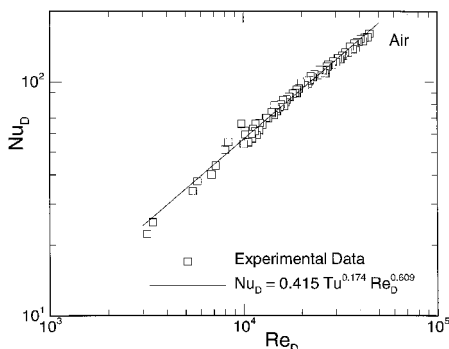


Fig. 3 Relationship between Nu_D and Re_D for experimental data.

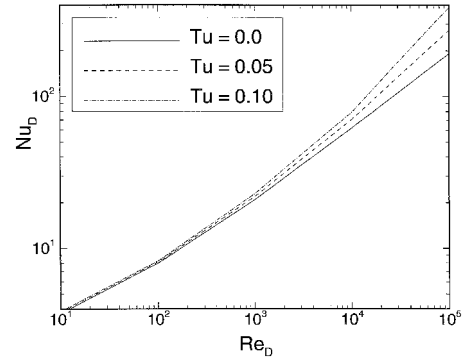


Fig. 4 Effect of Tu on the relationship between Nu_D and Re_D for approximate solution, Eq. (49).

Figure 3 shows the present data of Nu_D vs Re_D for forced convection heat transfer ($Pr = 0.71$) from an isothermal sphere. The effect of free convection is estimated to be 18% at $Re_D = 20,000$ and 5% at $Re_D = 80,000$. While radiation heat transfer over the same range of Reynolds number was between 3.4–0.8%, respectively.

The area-averaged Nusselt number can be calculated as follows:

$$Nu_D = hD/k = Q_{FC}D/kA\Delta T$$

where $\Delta T = T_s - T_\infty$, and the thermal conductivity of the fluid k is evaluated at the film temperature. Figure 4 shows the empirical relationship between the Nusselt and Reynolds numbers. The experimental results have been correlated as follows:

$$\begin{aligned} Nu_D &= 0.083Re_D^{0.709} \\ &= 0.415Tu^{0.174}Re_D^{0.609} \end{aligned} \quad (7)$$

for

$$5642 \leq Re_D \leq 56,420$$

$$0.012 \leq Tu \leq 0.049$$

The maximum percent difference between the experimental data and Eq. (7) is 6.6% and the rms percent difference is 3.05%.

In this study, the uncertainty in Nusselt and Reynolds numbers was investigated using the maximum error method and the orthogonal error method, respectively. It was concluded that the uncertainty in Nu_D was $\pm 2.9\%$ to $\pm 5.4\%$, and the uncertainty in Re_D was $\pm 2.1\%$ to $\pm 7.2\%$, with maximum errors in Nu_D and Re_D of $\pm 12.6\%$ and $\pm 8.54\%$, respectively, over the operating temperature range of 300–330 K.

Theoretical Analysis

Figure 1 shows a sphere of diameter D , which was maintained at an isothermal temperature T_s while immersed in a steady, uniform, incompressible fluid with constant properties. The bulk fluid was assumed to be at a constant temperature T_∞ and a uniform approach velocity V_∞ for a range of Prandtl numbers between zero and infinity.

An approximate analytical solution has been developed by Refai Ahmed and Yovanovich¹ in which the conventional form of the energy equation is used:

$$v_r \frac{\partial T}{\partial r} + v_\theta \frac{1}{r} \frac{\partial T}{\partial \theta} = \alpha \left[\frac{1}{r^2} \frac{\partial}{\partial r} \left(r^2 \frac{\partial T}{\partial r} \right) \right] \quad (8)$$

This particular form of the energy equation could not be used in the current analysis because of the significant turbulence intensity effect observed during experimental testing. The thermal diffusivity α in Eq. (8) fails to address the physical behavior encountered in turbulent flow problems.

The present investigation must consider the effect of the turbulence intensity. Therefore, the energy equation can be written using a Boussinesq approximation¹⁷ and assuming that negligible heat is dissipated inside the boundary layer:

$$\begin{aligned} \bar{v}_r \frac{\partial T}{\partial r} + \bar{v}_\theta \frac{1}{r} \frac{\partial T}{\partial \theta} &= \frac{1}{r^2} \frac{\partial}{\partial r} \left(\alpha^* r^2 \frac{\partial T}{\partial r} \right) \\ \text{LHS} &= \alpha^* \left[\frac{1}{r^2} \frac{\partial}{\partial r} \left(r^2 \frac{\partial T}{\partial r} \right) \right] + \frac{\partial T}{\partial r} \frac{\partial \alpha^*}{\partial r} \quad (9) \\ \text{RHS} \end{aligned}$$

The diffusivity α^* is the sum of the laminar diffusivity α and the turbulent diffusivity α_t . The turbulent thermal diffusivity is approximated as the turbulent kinematic viscosity ν_t , when the turbulent Prandtl number is equal to unity. Arpaci and Larsen¹⁸ reported values of the total thermal diffusivity between 1.0–0.9. For simplification of the present analysis the turbulent Prandtl number is considered to be equal to 1.0. ν_t is determined from Bejan¹⁹ through scaling analysis and using the mixing length theory of Prandtl²⁰ for flat plates. Bejan¹⁹ reported that

$$\alpha_t \approx \nu_t = K^2 y^2 \left| \frac{\partial \bar{u}}{\partial y} \right| \quad (10)$$

$$|u'| = Ky \frac{\partial \bar{u}}{\partial y} \quad (11)$$

Therefore

$$\alpha_t \approx \nu_t = Ky |u'| = Ky Tu V_\infty \quad (12)$$

where

$$\text{at } V_\infty \rightarrow 0 \quad \alpha^* = \alpha$$

$$\text{or } Tu \rightarrow 0 \quad \alpha = \alpha$$

For spheres $\nu_t \approx K(r - D/2)TuV_\infty$, where K is the constant in the mixing length, $l = Ky$.

The terms on the left side of Eq. (9) are approximated using a single equivalent term

$$\text{LHS} = \bar{v}_r \frac{\partial T}{\partial r} + \bar{v}_\theta \frac{1}{r} \frac{\partial T}{\partial \theta} \approx \frac{\bar{v}_e}{r} \frac{\partial T}{\partial \theta} \quad (13)$$

where \bar{v}_e will be determined later. This idea has been proposed by Oseen²¹ to linearize the inertia term for creeping flow, where he assumed the convective term to be $V_\infty \nabla \cdot \mathbf{v}$ (see Happel and Brenner²²). In addition the RHS of Eq. (9) can be simplified through scaling analysis as follows:

$$\begin{aligned} \text{RHS} &= (\alpha + \alpha_t) \frac{\partial^2 T}{\partial r^2} + \frac{\partial \alpha_t}{\partial r} \frac{\partial T}{\partial r} \\ &= \left[\alpha + K Tu V_\infty \left(r - \frac{D}{2} \right) \right] \frac{\Delta T}{(r - D/2)^2} \\ &\quad + K Tu V_\infty \frac{\Delta T}{(r - D/2)} \quad (14) \end{aligned}$$

Table 1 Prediction of α_t/α using flat plate information

Re_D^a	$Tu, \%^b$	α_t/α
100	0.13	4.15×10^{-4}
1,000	0.507	0.0512
10,000	1.905	0.60
100,000	7.16	7.23

^a D is the plate length in this table.

^b $Tu = 9.55 \times 10^{-3} Re_D^{0.577}$.

To obtain an estimate of (α_t/α) over the range of Reynolds numbers from 10^2 to 10^5 , one can use the flat plate information as follows:

$$\alpha_t \approx \nu_t \approx K \delta Tu V_\infty \quad (15)$$

where $\delta \sim x/\sqrt{Re_x}$ and $K \approx 0.45$ – 0.5 (von Kármán's constant), therefore

$$\alpha_t \approx 0.45 \cdot Pr \cdot \alpha \cdot Tu \cdot \sqrt{Re} \quad (16)$$

$$\text{for air } \alpha_t/\alpha \approx 0.3 \cdot Tu \cdot \sqrt{Re}$$

The prediction of α_t/α from the flat plate analysis for the range of Reynolds numbers between 10^2 – 10^5 is given in Table 1. One observes that α^* approaches α for small values of Tu and V_∞ , therefore, α^* can be considered a weak function of (r) , i.e., independent of r up to $Re_D = 10^4$.

Therefore, Eq. (9) is reduced to Eq. (17), where α^* is assumed to be constant in r direction.

$$\frac{\bar{v}_e}{r} \frac{\partial T}{\partial \theta} = \alpha^* \left[\frac{1}{r^2} \frac{\partial}{\partial r} \left(r^2 \frac{\partial T}{\partial r} \right) \right] \quad (17)$$

where Eq. (17) is limited to the range: $r \geq (D/2)$ and $0 \leq \theta \leq \pi$.

Equation (17) is then transformed to an equivalent transient heat conduction problem to find a suitable solution. Assuming that the flow particles are moving with a constant effective velocity \bar{v}_e around the body, the particles will take time Δt to travel a distant $r\Delta\theta$. Furthermore, for $\Delta\theta \rightarrow 0$ and $\Delta t \rightarrow 0$, one obtains

$$\bar{v}_e = r \frac{\partial \theta}{\partial t} \quad \text{where} \quad \frac{D}{2} \leq r \leq \delta + \frac{D}{2} \quad (18)$$

Thus, by substituting Eq. (18) into Eq. (17) the energy equation is written as follows:

$$\frac{\partial T^*}{\partial t} = \alpha^* \left[\frac{1}{r^2} \frac{\partial}{\partial r} \left(r^2 \frac{\partial T^*}{\partial r} \right) \right] \quad (19)$$

where

$$r \geq \frac{D}{2}, \quad 0 \leq t \leq \frac{\pi D}{2\bar{v}_e} \quad \text{and} \quad T^* = \frac{T - T_\infty}{T_s - T_\infty}$$

The solution to Eq. (19) can be obtained from Carslaw and Jaeger²³ and is given as

$$\begin{aligned} T^* &= \frac{D}{2} \frac{1}{r} \operatorname{erfc} \left(\frac{r - D/2}{2\sqrt{\alpha^* t}} \right) \bigg|_{t=(\theta D)/(2\bar{v}_e)} \\ &= \frac{D}{2} \frac{1}{r} \operatorname{erfc} \left[\frac{r - D/2}{2\sqrt{\alpha^* \theta D/(2\bar{v}_e)}} \right] \quad (20) \end{aligned}$$

The local Nusselt number is

$$Nu_D(\theta) = q_s(\theta)D/(T_s - T_\infty)k \quad (21)$$

where

$$\begin{aligned} q_s(\theta) &= -\rho C_p \alpha^*(T_s - T_\infty) \frac{\partial T^*}{\partial r} \bigg|_{r=D/2} \\ &= \frac{\rho C_p \alpha^*(T_s - T_\infty)}{D/2} + \frac{\rho C_p \alpha}{\sqrt{\pi}} \frac{(T_s - T_\infty)}{\sqrt{\alpha^* D \theta/2} \bar{v}_e} \end{aligned} \quad (22)$$

The transient conduction solution provides an analytical solution for the local Nusselt number that consists of the linear sum of the local boundary-layer term and the constant term corresponding to the diffusive limit ($Re_D \rightarrow 0$). The area-averaged Nusselt number $Nu_D = (1/A) \int_A Nu_D(\theta) dA$, is given by

$$Nu_D = (2\alpha^*/\alpha) + (0.714\alpha^*/\alpha)\sqrt{D\bar{v}_e/\alpha^*} \quad (23)$$

The diffusive term in the previous equation is multiplied by (α^*/α) . This factor α^*/α goes to unity at the diffusive limit $Re_D \rightarrow 0$. Furthermore, to complete the analysis, \bar{v}_e can be defined for the limiting cases of $Pr \rightarrow \infty$ and $Pr \rightarrow 0$, allowing an interpolation function to be obtained, providing a relationship valid for all Prandtl numbers.

Despite the fact that flow separation can occur at high Reynolds numbers, the present analysis is based on the assumption that the flow does not separate at any point over the surface of the sphere for the full range of Reynolds numbers examined. We will proceed with the analysis and compare the results with available experimental results (which include the separation effects), to determine the capabilities of the present model.

\bar{v}_e^∞ at $Pr \rightarrow \infty$

First, one can consider high Prandtl number fluids. Scaling analysis is applied to the continuity, momentum, and energy equations to determine the area-averaged effective velocity. Assume that the hydrodynamic boundary layer (HBL), δ , is very thin, i.e., $D/2 + \delta \approx D/2$ (see Fig. 1), where $Re_D \gg 1$. It is also assumed that the flow outside of the hydrodynamic boundary layer is effectively inviscid. Thus, the local velocity at the edge of the HBL is equal to $\bar{v}_\theta(D/2 + \delta) = V(\theta)$, where $V(\theta)$ is the solution to the inviscid flow problem, as shown in Fig. 1. The continuity equation in an axisymmetric incompressible turbulent flow inside the HBL can be approximated as follows:

$$\frac{2}{r} \bar{v}_r + \frac{\partial \bar{v}_r}{\partial r} + \frac{1}{r} \frac{\partial \bar{v}_\theta}{\partial \theta} + \frac{\cot \theta}{r} \bar{v}_\theta = 0 \quad (24)$$

Using scaling analysis (the scaling analysis rules are stated in Bejan²⁴) on the continuity equation within the HBL gives the relationship:

$$\frac{4\bar{v}_r|_{D/2}}{D} + \frac{\bar{v}_r|_{\delta+D/2} - \bar{v}_r|_{D/2}}{\delta} + \frac{2}{D} \frac{\bar{v}_\theta}{\theta} + \frac{2}{D} \frac{\bar{v}_\theta}{\theta} \sim 0$$

With $\bar{v}_\theta|_{\delta+D/2} = V(\theta)$ and the inviscid flow solution with $\bar{v}_r|_{D/2} = 0$, we obtain

$$\bar{v}_r|_{\delta+D/2} \sim 2 \frac{\delta}{D} \frac{V(\theta)}{\theta} \quad (25)$$

Applying scaling analysis on the continuity equation inside the thermal boundary layer (TBL), gives the relationship:

$$\bar{v}_r|_{\delta_T+D/2} \sim 2 \frac{\delta_T^2}{D\delta} \frac{V(\theta)}{\theta} \quad (26)$$

where it is assumed that the ratio $V/V(\theta)$ is approximately equal to δ_T/δ , i.e., the flow has a linear velocity distribution (as shown in Fig. 1).

One can assume that the flow outside the boundary layer is inviscid. Therefore, the pressure term in the momentum equation (θ direction) can be approximated as

$$\frac{V(\theta)}{r} \frac{\partial V(\theta)}{\partial \theta}$$

by using the Bernoulli equation. The momentum equation in a steady axisymmetric flow along the body becomes

$$\bar{v}_r \frac{\partial \bar{v}_\theta}{\partial r} + \frac{\bar{v}_\theta}{r} \frac{\partial \bar{v}_\theta}{\partial \theta} \approx \frac{V(\theta)}{r} \frac{\partial V(\theta)}{\partial \theta} + \frac{1}{r^2} \frac{\partial}{\partial r} \nu^* r^2 \frac{\partial \bar{v}_\theta}{\partial r} \quad (27)$$

Using scaling analysis on the momentum equation inside the HBL with Eq. (24) gives the following relationship:

$$\frac{2\delta V^2(\theta)}{D\delta\theta} + \frac{2V^2(\theta)}{D\theta} \approx \frac{2V^2(\theta)}{D\theta} + \nu^* \frac{V(\theta)}{\delta^2} \quad (28)$$

The local hydrodynamic boundary-layer thickness can then be written as

$$\frac{\delta}{D} \sim \sqrt{\frac{\theta \nu^*/\nu}{2Re_D(\theta)}} \quad (29)$$

where $Re_D(\theta) = DV(\theta)/\nu$.

Applying scaling analysis to the energy equation, Eq. (17), and keeping in mind that $D/2 \gg \delta_T$ and $v_\theta|_{\delta_T} = V = [(\delta_T/\delta) \cdot V(\theta)]$, one can obtain that

$$\frac{2\delta_T^2}{D\delta} \frac{V(\theta)}{\theta} \frac{\Delta T}{\delta_T} + \frac{\delta_T V(\theta) \Delta T}{\delta \theta D/2} \sim \frac{\alpha^* \Delta T}{\delta_T^2} \quad (30)$$

The two convective terms on the LHS of Eq. (30) have a similar order of magnitude; therefore, it can be equated to one of the convective terms to the diffusion term as follows:

$$\frac{\delta_T V(\theta) \Delta T}{\delta \theta D/2} \sim \frac{\alpha^* \Delta T}{\delta_T^2} \quad (31)$$

The local dimensionless thermal boundary-layer thickness is given by

$$\frac{\delta_T}{D} \sim \left(\frac{\alpha^*}{\nu^*} \right)^{1/3} \sqrt{\frac{\theta \nu^*/\nu}{2Re_D(\theta)}} \quad (32)$$

Comparing Eq. (32) with Eq. (29) one can find that

$$\frac{\delta_T}{\delta} \sim \frac{V}{V(\theta)} \sim \left(\frac{\alpha^*}{\nu^*} \right)^{1/3} \quad (33)$$

This result will be used subsequently to define \bar{v}_e^∞ .

The local effective velocity $\bar{v}_e^\infty(\theta)$ for large Prandtl numbers fluids will be obtained from momentum flux balances through the thermal boundary-layer thickness. The momentum flux inside the thermal boundary layer is

$$\frac{\rho}{\delta_T} \int_0^{\delta_T} \bar{v}_\theta (V - \bar{v}_\theta) dy \quad (34)$$

On the other hand, if we determine the momentum flux by assuming that the flow has a uniform local effective velocity,

$v_e^\infty(\theta)$ is constant in the y direction and variable in the x direction, we have

$$\frac{\rho}{\delta_r} \int_0^{\delta_r} v_e^\infty(\theta)(V - \bar{v}_\theta) dy \quad (35)$$

Equating Eqs. (34) and (35) and solving for the local effective velocity we obtain

$$v_e^\infty(\theta) = V \frac{\int_0^{\delta_r} \frac{\bar{v}_\theta}{V} (V - \bar{v}_\theta) dy}{\int_0^{\delta_r} (V - \bar{v}_\theta) dy} \quad (36)$$

which can be expressed in terms of the momentum and displacement thicknesses as follows:

$$v_e^\infty(\theta) \sim V(\theta) \cdot \frac{\delta_r}{\delta} \cdot \frac{\delta_M^T}{\delta_D^T} \sim V(\theta) \cdot \left(\frac{\alpha^*}{\nu^*} \right)^{1/3} \cdot \frac{\delta_M^T}{\delta_D^T} \quad (37)$$

For convenience of the subsequent analysis, a similarity parameter $\eta = y/\delta_r$ is introduced. This allows one to express the momentum and displacement thicknesses in the following forms:

$$\delta_M^T = \delta_r \int_0^1 \frac{\bar{v}_\theta}{V} \left(1 - \frac{\bar{v}_\theta}{V} \right) d\eta \quad (38)$$

$$\delta_D^T = \delta_r \int_0^1 \left(1 - \frac{\bar{v}_\theta}{V} \right) d\eta \quad (39)$$

Clearly, these important hydrodynamic thicknesses depend on the velocity distribution within the TBL. One may assume that \bar{v}_θ is a power-law function of y to have a general form for the velocity profiles at different Reynolds numbers, i.e., $\bar{v}_\theta/V = (y/\delta_r)^{\gamma_D}$ or $\bar{v}_\theta/V = \eta^{\gamma_D}$, where $0 \leq \eta \leq 1$.

Introducing the power-law velocity distribution into Eqs. (38) and (39) and integrating, one obtains the relationship between the momentum and displacement thicknesses in terms of the power-law exponent (γ_D):

$$\frac{\delta_M^T}{\delta_D^T} = \frac{1}{2\gamma_D + 1} \quad (40)$$

Therefore, the local effective velocity from Eq. (37) with Eq. (40) is

$$v_e^\infty(\theta) \sim \frac{V(\theta)}{(2\gamma_D + 1)} \left(\frac{\alpha^*}{\nu^*} \right)^{1/3} \quad (41)$$

The area-averaged effective velocity is defined as

$$\bar{v}_e^\infty \sim \frac{1}{(2\gamma_D + 1)} \left(\frac{\alpha^*}{\nu^*} \right)^{1/3} \cdot \frac{1}{A} \int_A V(\theta) dA \quad (42)$$

Furthermore, the ideal flow solution can be used to represent the flow in the region outside of the boundary layer; therefore,

$$\bar{v}_\theta|_{\delta+D/2} = V(\theta) = 1.5V_\infty \sin \theta \quad (43)$$

After substitution of Eq. (43) into Eq. (42), we find that the area-averaged effective velocity as $Pr \rightarrow \infty$ is given by

$$\bar{v}_e^\infty \sim \frac{1.178V_\infty}{(2\gamma_D + 1)} \left(\frac{\nu^*}{\alpha^*} \right)^{1/3} \quad (44)$$

\bar{v}_e^0 at $Pr \rightarrow 0$

If one considers that the viscosity is very small, i.e., $Pr \rightarrow 0$, and $Re_D \gg 1$. The HBL, δ , is very small and the TBL, δ_r , is very large relative to δ ; therefore, at the edge of the TBL we have

$$\bar{v}_\theta|_{(\delta+D/2)} = \frac{V_\infty}{2} \cdot \left[2 + \left(\frac{D}{2(\delta + D/2)} \right)^3 \right] \sin \theta \quad (45)$$

Equation (45) can be reduced to $\bar{v}_\theta|_{(\delta+D/2)} = V = 1.5V_\infty \sin \theta$, where $\delta \ll D/2$.

Therefore, the local velocity at arbitrary θ will be considered uniform across the TBL. As a result, $v_e^0(\theta) = V$, as shown in Fig. 1 [V is the local maximum velocity at the edge of the TBL and $v_e^0(\theta)$, is the local effective velocity at $Pr \rightarrow 0$]. The area-mean effective velocity is

$$\bar{v}_e^0 = \frac{1}{A} \int_A V dA = 1.178V_\infty \quad (46)$$

\bar{v}_e for All Pr

At this point the effective velocity has been determined for the two limiting cases where $Pr \rightarrow \infty$ and $Pr \rightarrow 0$. To develop an expression for \bar{v}_e that is valid for all Prandtl numbers, the Churchill and Usagi²⁵ blending technique will be used. The area-averaged effective velocity can now be expressed, as recommended by Refai Ahmed and Yovanovich,¹ in the following form:

$$\bar{v}_e = \frac{\bar{v}_e^\infty}{[1 + (\bar{v}_e^\infty/\bar{v}_e^0)^n]^{1/n}} \quad (47)$$

Substituting \bar{v}_e^0 and \bar{v}_e^∞ into Eq. (47) gives the effective velocity valid for all Prandtl numbers in terms of the power-law parameter γ_D and the blending parameter n

$$\frac{\bar{v}_e}{V_\infty} = \frac{1.178/[(2\gamma_D + 1)(\nu^*/\alpha^*)^{1/3}]}{(1 + [1/(2\gamma_D + 1)(\nu^*/\alpha^*)^{1/3}]^n)^{1/n}} \quad 0 < Pr < \infty \quad (48)$$

where $0 \leq \gamma_D \leq 1$. The constant n will be determined in the following section.

Results and Discussion

To determine an analytical expression for Nu_D , one must substitute Eq. (48) into Eq. (23). Nu_D becomes

$$Nu_D = \left(1 + Pr \frac{\alpha_t}{\nu} \right) \cdot \left[2 + \frac{0.775 Re_D^{0.5} \left[\frac{(1/Pr) + (\alpha_t/\nu)}{1 + (\nu_t/\nu)} \right]^{1/6}}{\sqrt{(2\gamma_D + 1) \left(\frac{1}{Pr} + \frac{\nu_t}{\nu} \right) \left(1 + \left\{ \frac{(1/Pr) + (\alpha_t/\nu)}{(2\gamma_D + 1)^3 [1 + (\nu_t/\nu)]} \right\}^{n/3} \right)^{1/2n}} \right] \quad (49)$$

The numerical range of n is between 1 and ∞ . However, Eq. (49) changes significantly in the range of $1 \leq n \leq 3$. In contrast, the range of $n > 3$ does not change Eq. (49) with respect to $n = 3$. Therefore, the region of interest of n is between 1–3. One can obtain linear superposition at $n = 1$, but this does not give the best fit. On the other hand, it is found that $n = 3$ gives the best fit by matching Eq. (49) with the present air data and $\gamma_D = 1/(1 + Re_D^{1.25})^{1/5}$ (Refai Ahmed and Yovanovich^{1,26}). As mentioned before, the turbulent Prandtl number

$$\begin{aligned}
 Nu_D = & \text{I} \quad 2 + \frac{0.775 Re_D^{0.5} \left[\frac{(1/Pr) + (\alpha_i/\nu)}{1 + (\nu_i/\nu)} \right]^{1/6}}{\sqrt{(2\gamma_D + 1) \left(\frac{1}{Pr} + \frac{\nu_i}{\nu} \right) \left(1 + \left\{ \frac{(1/Pr) + (\alpha_i/\nu)}{(2\gamma_D + 1)^3 [1 + (\nu_i/\nu)]} \right\} \right)^{1/6}}} \\
 & \text{II} \\
 & + \left(Pr \frac{\alpha_i}{\nu} \right) \cdot 2 + \frac{0.775 \left(Pr \frac{\alpha_i}{\nu} \right) \cdot Re_D^{0.5} \left[\frac{(1/Pr) + (\alpha_i/\nu)}{1 + (\nu_i/\nu)} \right]^{1/6}}{\sqrt{(2\gamma_D + 1) \left(\frac{1}{Pr} + \frac{\nu_i}{\nu} \right) \left(1 + \left\{ \frac{(1/Pr) + (\alpha_i/\nu)}{(2\gamma_D + 1)^3 [1 + (\nu_i/\nu)]} \right\} \right)^{1/6}}} \\
 & \text{III} \\
 & \text{IV}
 \end{aligned} \tag{54}$$

ν_i/α_i is set to unity. Therefore, $\alpha_i = \nu_i \approx K[r - (D/2)]TuV_\infty$, where $(r - D/2)$ is δ , which is defined in Eq. (29). Therefore,

$$\frac{\nu_i}{\nu} = K Tu \delta \frac{V_\infty}{\nu} = K Tu Re_D \sqrt{\frac{\theta[1 + (\nu_i/\nu)]}{2 Re_D \delta(\theta)}}$$

which can be rewritten:

$$\begin{aligned}
 \frac{\nu_i/\nu}{\sqrt{1 + (\nu_i/\nu)}} &= K Tu Re_D \sqrt{\frac{\theta}{2 Re_D \delta(\theta)}} \\
 &= K Tu Re_D \sqrt{\frac{\theta}{DV(\theta)/\nu}} = \Phi \cdot \sqrt{\frac{\theta}{1.5 \sin \theta}} \tag{50}
 \end{aligned}$$

The previous equation is a function of θ . Therefore, the average value of ν_i/ν over the entire surface can be determined in the two limits: $\nu_i/\nu \rightarrow \infty$ and $\nu_i/\nu \rightarrow 0$.

Finally, the general form of ν_i/ν can be obtained using blending techniques as shown next:

$\nu_i/\nu \rightarrow \infty$:

$$\frac{\nu_i}{\nu} = \Phi^2 \frac{1}{A} \int \int_A \frac{\theta}{1.5 \sin \theta} dA = 1.645 K^2 Tu^2 Re_D \tag{51}$$

$\nu_i/\nu \rightarrow 0$:

$$\frac{\nu_i}{\nu} = \Phi \frac{1}{A} \int \int_A \sqrt{\frac{\theta}{1.5 \sin \theta}} dA = 1.668 K Tu \sqrt{Re_D} \tag{52}$$

$0 < \nu_i/\nu < \infty$:

$$\frac{\nu_i}{\nu} = [(1.668 K Tu \sqrt{Re_D})^3 + (1.645 K^2 Tu^2 Re_D)^3]^{1/3} \tag{53}$$

K is estimated to be between 0.3–0.4 for flat plates, as reported by Arpacı and Larsen.¹⁸ In addition, Smith and Kueth²⁷ recommended that $K = 0.164$ for the circular cylinder. There-

fore, it was found that $K = 0.05$ to give the best fit by matching Eq. (49) with the present experimental air data.

One can verify the previous flat plate approximation of α_i/α by using Eq. (53). Table 2 shows the estimation of α_i/α (where $\alpha_i/\alpha = Pr \nu_i/\nu$) in the range of $10^2 \leq Re_D \leq 10^5$ and confirms the assumption that α^* is a weak function of r in that range.

One can expand Eq. (49) to four terms; term I is the diffusive limit, and terms II–IV are the boundary-layer regime with turbulent intensity effects as follows:

Also, one can observe that the terms III and IV vanish when α_i or $\nu_i \rightarrow 0$, i.e., $Tu \rightarrow 0$. However, the second term is reduced to the following form:

$$\frac{0.775 Re_D^{0.5} Pr^{1/3}}{\sqrt{(2\gamma_D + 1) [(2\gamma_D + 1)^3 + (1/Pr)]^{1/6}}} \tag{55}$$

The sum of the diffusive term I and Eq. (55) is identical to the solution of Refai Ahmed and Yovanovich.¹ Figure 4 shows the relationship between Nu_D and Re_D for several values of the turbulence intensity in the range $0 \leq Tu \leq 0.1$. One finds that the effect of Tu on Nu_D is negligible for low Reynolds numbers $Re_D \leq 100$. Furthermore, for $Tu = 0.01$, the effect of Tu on Nu_D is less than 3% for $Re_D \leq 10^4$. By contrast, this effect is more significant for high Tu or Re_D . For example, $\Delta Nu/Nu$ is 100% at $Re_D = 10^5$ and $Tu = 0.1$ and 9.5% at $Re_D = 10^3$ and $Tu = 0.1$. Also, Fig. 4 shows that the relationship between Nu_D and Re_D at $Tu = 0$, Eq. (54), is identical to the Refai Ahmed and Yovanovich¹ solution. Thus, the present solution, at $Tu = 0$ and $0 \leq Re_D < 10^5$, is found to be in very good agreement with many previous studies such as Refs. 12 and 28–30 (more detailed comparisons of this case can be found in Refai Ahmed and Yovanovich¹).

Figure 5 shows a comparison between the present experimental results and the upper and lower bounds of Nu_D vs Re_D , calculated using the approximate analytical solution, Eq. (49), for turbulence intensities corresponding to the range of Tu (0.0–0.045) found in testing. Since each of the data points is a function of Tu , as shown in Eq. (7), a single line cannot be passed through all of the data points; however, the experimental data is clearly bounded by the curves corresponding to $Tu = 0$ and 0.045. The maximum difference between the ex-

Table 2 Prediction of α_i/α using Eq. (53)

Re	$Tu, \%^a$	α_i/α
100	0.13	5.68×10^{-4}
1,000	0.507	6.74×10^{-3}
10,000	1.905	7.95×10^{-2}
100,000	7.16	1.79

^a $Tu = 9.5 \times 10^{-3} Re_D^{0.577}$.

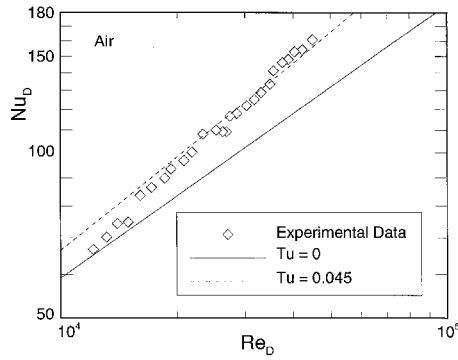


Fig. 5 Comparison between data and proposed model, Eq. (49).

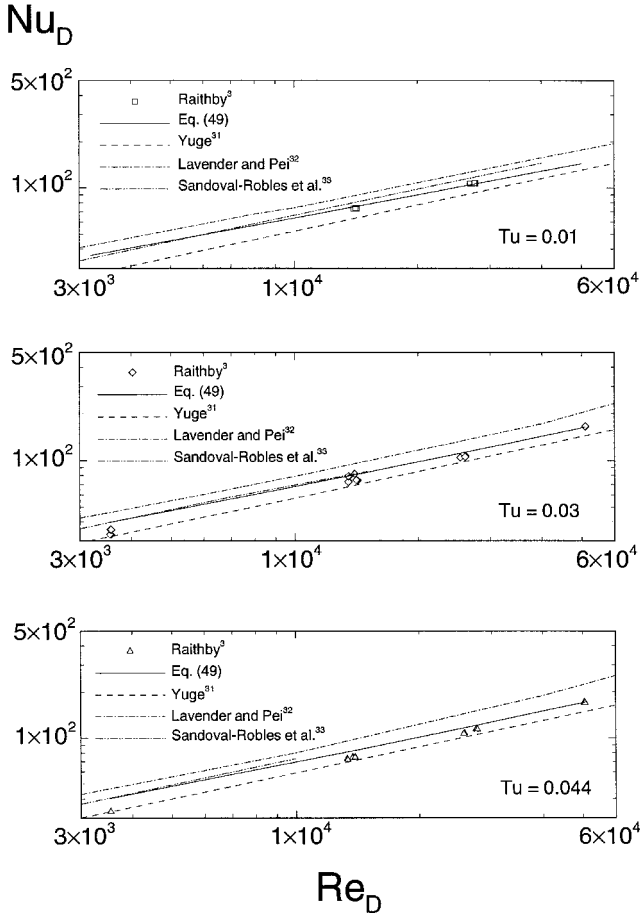


Fig. 6 Comparison between previous studies and Eq. (49).

perimental data and the approximate solution is 7.7% at $Re_D \approx 11,000$. It is expected that at $Re_D \approx 11,000$, the experimental error is larger than the error at $Re_D \approx 5 \times 10^4$. Figure 6 also shows the comparison between the present model, Eq. (49), and the experimental data of Raithby³ in the following ranges: $0.01 \leq Tu \leq 0.044$ and $3000 < Re_D < 6 \times 10^4$. The maximum difference of approximately 17% between the Raithby data³ and the proposed model occurs at low Reynolds number, and the average difference between the present investigation and the Raithby data³ is within 8%. The present model also compared against the correlations of the experimental data of Yuge,³¹ Lavender and Pei,³² and Sandoval-Robles et al.³³ These correlations are as follows.

Yuge³¹:

$$Nu_D = 2 + 0.0339Re_D^{0.585}Tu^{0.085} \quad Re_D \cdot Tu < 7000 \quad (56)$$

Lavender and Pei³²:

$$Nu_D = 2 + 0.629Re_D^{0.535}Tu^{0.035} \quad Re_D \cdot Tu < 1000 \quad (57)$$

$$Nu_D = 2 + 0.145Re_D^{0.75}Tu^{0.25} \quad Re_D \cdot Tu > 1000$$

Sandoval-Robles et al.³³:

$$Sh_D = 0.549Re_D^{0.566}Tu^{0.066}Sc^{1/3} \quad 12 < Re_D \cdot Tu < 600 \quad (58)$$

Figure 6 shows that the average differences between Eq. (49) and Yuge³¹ Lavender and Pei,³² and Sandoval-Robles et al.³³ are 10, -28.8, and -11.23%, respectively.

Summary and Conclusions

An approximate analytical solution, supported by an experimental investigation, is presented for predicting forced convection heat transfer from isothermal spheres. This model is valid for a range of Reynolds numbers between $0 \leq Re_D \leq 10^5$ and a full range of Prandtl numbers between zero and infinity. In addition, the present study examined the effect of turbulence intensity on the heat transfer results. The approximate analytical solution is found to be in very good agreement with the present experimental results and the data of Raithby³ and the correlations of the experimental data of Yuge³¹ and Sandoval-Robles et al.³³ Furthermore, in the present study, it is concluded that the main reason for the differences in the exponent of Re_D in the previous studies is because of their curve-fitting data in various ranges of Re_D , which have different velocity profiles and turbulence intensities.

Acknowledgments

The authors wish to acknowledge the financial support of the Natural Sciences and Engineering Research Council of Canada under Grant A7455. The first author also wishes to acknowledge the financial support of R—Theta Inc., Mississauga, Canada.

References

- Refai Ahmed, G., and Yovanovich, M. M., "Approximate Analytical Solution of Forced Convection Heat Transfer from Isothermal Spheres for All Prandtl Numbers," *Journal of Heat Transfer*, Vol. 116, No. 4, 1994, pp. 838–843.
- Loitzianski, L. G., and Schwab, B. A., Central Aerodynamics Hydrodynamics Inst., Rept. 329, Russia, 1935.
- Raithby, G. D., "The Effect of Turbulence and Support Position on the Heat Transfer from Flow Around Spheres," Ph.D. Dissertation, Univ. of Minnesota, MN, 1967.
- Maisel, D. S., and Sherwood, T. K., "Effect of Air Turbulence on Rate of Evaporation of Water," *Chemical Engineering Progress*, Vol. 46, No. 1, 1950, pp. 172–175.
- Rae, W. H., and Pope, A., *Low-Speed Wind Tunnel Testing*, 2nd ed., Wiley, New York, 1984.
- Clift, R., Grace, J. R., and Weber, M. E., *Bubbles, Drops and Particles*, Academic, New York, 1978.
- Refai Ahmed, G., "The Effect of Screens Upon Wind Tunnel Turbulence," Dept. of Mechanical Engineering, Univ. of Waterloo/Microelectronics Heat Transfer Lab., TR9312-G44, Waterloo, ON, Canada, 1993.
- Hassani, A. V., "An Investigation of Free Convection Heat Transfer from Bodies of Arbitrary Shapes," Ph.D. Dissertation, Dept. of Mechanical Engineering, Univ. of Waterloo, Waterloo, ON, Canada, 1987.
- Mack, B., "Natural Convection from an Isothermal Cube on a Vertical Plate," M.S. Thesis, Mechanical Engineering Dept., Univ. of Waterloo, Waterloo, ON, Canada, 1991.
- Refai Ahmed, G., "Experimental and Approximate Analytical Study of Forced Convection Heat Transfer from Isothermal Body Shapes," Ph.D. Dissertation, Mechanical Engineering Dept., Univ. of Waterloo, Waterloo, ON, Canada, 1994.
- Yovanovich, M. M., and Vanoverbeke, C. A., "Combined Natural and Forced Convection Heat Transfer from Isothermal Sphere," AIAA Paper 88-2618, June 1988.
- Yuge, T., "Experiments on Heat Transfer from Spheres Including Combined Natural Convection," *Journal of Heat Transfer*, Vol. 82, No. 2, 1960, pp. 214–220.

¹³Raithby, G. D., and Hollands, K. G. T., "Analysis of Heat Transfer by Natural Convection (or Film Condensation) for Three Dimensional Flows," *Proceedings of the 6th International Heat Transfer Conference* (Toronto, Canada), Vol. 2, Hemisphere, Washington, DC, 1978, pp. 187-192.

¹⁴Steinberger, L., and Treybal, R., "Mass Transfer from a Solid Sphere to a Flowing Liquid Stream," *AIChE Journal*, Vol. 6, No. 2, 1960, pp. 227-232.

¹⁵Churchill, S. W., "Comprehensive Theoretically Based, Correlating Equations for Free Convection from Isothermal Spheres," *Chemical Engineering Communications*, Vol. 24, Nos. 4-6, 1983, pp. 339-352.

¹⁶Jafarpur, K., "Analytical and Experimental Study of Laminar Free Convection Heat Transfer from Isothermal Convex Bodies of Arbitrary Shapes," Ph.D. Dissertation, Dept. of Mechanical Engineering, Univ. of Waterloo, Waterloo, ON, Canada, 1992.

¹⁷Boussinesq, J., "Théorie l'Ecoulement Tourbillant," *Mem. Prés. Acad. Sci.*, XXIII, 46, Paris, 1877.

¹⁸Arpaci, V. S., and Larsen, P. S., *Convection Heat Transfer*, Prentice-Hall, Englewood Cliffs, NJ, 1984.

¹⁹Bejan, A., *Convective Heat Transfer*, Wiley, New York, 1984.

²⁰Prandtl, L., "Über die ausgebildete Turbulenz," *Zeitschrift für Angewandte Mathematik und Mechanik*, Vol. 5, 1925, pp. 136-139.

²¹Oseen, C. W., *Hydrodynamik*, Akademische Verlag, Leipzig, Germany, 1927.

²²Happel, J., and Brenner, H., *Low Reynolds Number Hydrodynamics*, 2nd ed., Noordhoff International, Leyden, The Netherlands, 1973.

²³Carslaw, H. S., and Jaeger, J. C., *Conduction of Heat in Solids*, 2nd ed., Clarendon, Oxford, England, UK, 1959.

²⁴Bejan, A., "The Method of Scale Analysis: Natural Convection

in Fluids," *Natural Convection Fundamentals and Applications*, edited by S. Kakac, W. Aung, and K. Viskanta, Hemisphere, New York, 1985, pp. 75-94.

²⁵Churchill, S. W., and Usagi, R., "A General Expression for the Correlation of Rates of Transfer and Other Phenomena," *AIChE Journal*, Vol. 18, No. 5, 1972, pp. 1121-1132.

²⁶Refai Ahmed, G., and Yovanovich, M. M., "Analytical Method for Forced Convection from Flat Plates, Circular Cylinders, and Spheres," *Journal of Thermophysics and Heat Transfer*, Vol. 9, No. 3, 1995, pp. 516-523.

²⁷Smith, M. C., and Kueth, A., "Effects of Turbulence on Laminar Skin Friction and Heat Transfer," *Physics of Fluids*, Vol. 9, No. 12, 1966, pp. 2337-2344.

²⁸Frössling, N. M., "The Evaporation of Falling Drops," *Gerlands Beitrage zur Geophysik*, Vol. 52, 1938, pp. 170-216.

²⁹Kramers, H., "Heat Transfer from Spheres to Flowing Media," *Physica*, Vol. 12, Nos. 2, 3, 1946, pp. 61-81.

³⁰Churchill, S. W., "A Comprehensive Correlating Equation for Laminar, Assisting, Forced and Free Convection," *AIChE Journal*, Vol. 23, No. 1, 1977, pp. 10-16.

³¹Yuge, T., "Experiments on Heat Transfer of Spheres—Report 3 (Influence of Free Stream Turbulence at Higher Reynolds Numbers)," *Rep. Inst. High Sp. Mech. Japan*, Vol. 11, 1959, pp. 209-230.

³²Lavender, W. I., and Pei, D. C. T., "The Effect of Fluid Turbulence on the Rate of Heat Transfer from Spheres," *International Journal of Heat and Mass Transfer*, Vol. 9, No. 3, 1967, pp. 529-539.

³³Sandoval-Robles, J. G., Delmas, H., and Couderc, J. P., "Influence of Turbulence on Mass Transfer Between a Liquid and a Solid Sphere," *AIChE Journal*, Vol. 27, No. 5, 1981, pp. 819-823.